ORIENTAL JOURNAL OF CHEMISTRY
An International Open Free Access, Peer Reviewed Research Journal
www.orientjchem.org
Est. 1984
ISSN: 0970-020 X
CODEN: OJCHEG
2018, Vol. 34, No.(4):
Pg. 1832-1841

Impervious Nature of Al_2O_3-PANI Composite Against Corrosion on Mild Steel in Strong Acidic Environment

P. KAMATCHI SELVARAJ*, S. SIVAKUMAR and S. SELVARAJ

Department of Chemistry, Government Arts College for Men (AUT), Nandanam, Chennai – 35, India.
*Corresponding author E-mail: porbal96@gmail.com

http://dx.doi.org/10.13005/ojc/3404017

(Received: June 19, 2018; Accepted: July 11, 2018)

ABSTRACT

Solubility problem of composite in aqueous medium is resolved on adding Al_2O_3 during the oxidative polymerization of aniline using ammonium peroxydisulphate as an oxidant and sodium salt of dodecyl bezenesulphonic acid as surfactant and dopant at 273 K temperature. The yielded water soluble Al_2O_3-PANI composite is confirmed by comparing the FTIR, XRD and SEM recorded spectra with previously reported one. Gravimetric method exposes that the prepared composite is having confrontation against corrosion. Only a slight change in efficiency on continuous exposure up to eight hours is observed. OCP data are transformed in to potential graph to exposes the invincibility of the composite against corrosion. Measurement of potentiodynamic polarization and EIS studies also confirms the defiance against corrosion.

Keywords: Al_2O_3-Polyaniline (PANI), Mild steel, OCP, Potentiodynamic polarization, EIS.

INTRODUCTION

Metal working industries suffers mishap due to chemical or electrochemical attack on metal. Metal corrosion is a resolute threat to national economy and industry design[1,2]. It is miserable that corrosion can't be completely eradicated, as it is a natural process. Corrosion activities may be slow downed by other dynamic and/or substitute mechanisms. The undeniable methods include cathodic protection[3,4], protective coating[5] and addition of inhibitors[6]. Most of the protective coating layers lost their identity on prolonged exposure to corrosive environment[7-9]. Corrosion resistive performance of epoxy coatings were improved on insertion of TiO_2 nanomaterials[10,11]. It is a well known fact that corrosion of aluminum utensils is prevented due to the formation of protective Al_2O_3 layer on the surface of aluminum. Utility of Al_2O_3 have been found in the activities of catalyst[12], retardant for fire[13], absorbent[14] and filler[15]. Stability against chemical action, good conducting property, idiosyncratic doping behavior of polyaniline and other applications of it in energy storage and sensors attracted significantly to employ it as inhibiting material[16-18]. The structural morphology, thermal property and conductivity of PANI varied on insertion of TiO_2 and Al_2O_3[19,20]. Reinforced dielectric properties have been

noticed for Al_2O_3-PANI compositie.[20,21] Usage of solid Al_2O_3-PANI showed high value for dielectric property and impedance with very high Z" values[22]. All above observations stimulated to synthesis water soluble composite (Al_2O_3-PANI) and to evolve its capacity to diminish corrosion of carbon steel in strong acidic environment.

MATERIALS AND INSTRUMENTATION

Materials

AR grade monomer (aniline) was procured from Merck Ltd. After adding a pinch of zinc dust, it was purified by distillation to employ for polymerization. Phosphoric acid, Al_2O_3, ammonium peroxydisulphate (APS) and sodium salt of (DBSA) chemicals with AR grade purchased from Merck Ltd. were used without purification.

Instrumentation

The infrared spectrum, in the frequency range of 4000-450 cm^{-1}, was recorded by Perkin-Elmer 337 spectrometer. The XRD and SEM spectra were registered in Rigaku Maniflex diffractometer (Japan) and JSM-6390 Scanning Electron Microscope respectively. Potentiodynamic polarization studies and impedance measurements were documented in ECLAB 10.37 model. To observe the OCP values, CHI electrochemical analyzer instrument 1200B model was adopted.

EXPERIMENTAL

Synthesis of Al_2O_3-Polyaniline composite

Al_2O_3-PANI composite was synthesized by modified in-situ chemical oxidative polymerization method[23-25]. Aniline (18.6g) was added to 1M solution of Phosphoric acid (200ml) and stirred for half-an-hour. Solution prepared by dispersing required amount of Al_2O_3 in100 ml of 0.1M DBSA using 42 kHz oscillation frequency for 45 min. in a sonicator was mixed with aniline solution. The mixture was kept under constant stirring for two hours at 273 K along with addition of 200 ml of 1M APS solution in drops. Complete polymerization was achieved by stirring the above mixture for another three hours. The product (dark green in color) obtained was filtered, washed with deionized water, acetone, and dried in hot air oven at 55°C for 24 hours.

RESULTS AND DISCUSSION

Characterization of Al_2O_3-PANI composite

FTIR Analysis

The peak appears at 613 cm^{-1} in the FTIR spectrum of Al_2O_3 [Fig. 1(a)] was assigned to Al-O stretching vibration and the peak arises around 3460 cm^{-1} was ascribed to O-H vibration mode[26,27]. The bands appear in the FTIR spectrum of PANI [Fig. 1(b)] around 1562 cm^{-1} and 1447 cm^{-1} are due to stretching vibration of quinoid and benzenoid rings. The bands emerge about 1230 cm^{-1} and 1033 cm^{-1} are ascribed to C-N stretching vacillation[28,29]. The N-H stretching of secondary amine fetch up near 3400 cm^{-1}.

The FTIR spectrum of Al_2O_3-PANI composite [Fig. 1(c)] consist of the peaks due to Al_2O_3 and PANI with small blue or red shift. The O-H stretching of Al_2O_3 appears at 3490 cm^{-1}. The C=C stretching mode of quinoid rings occur around 1550 cm^{-1} and 1490 cm^{-1}. The Al-O stretching emerge at 508 cm^{-1}. Above results implies that the PANI has been coated over the surface of Al_2O_3 [22,30,31].

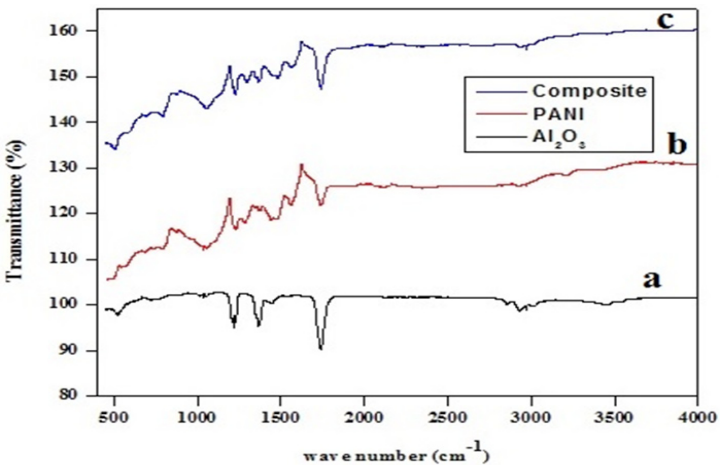

Fig. 1. FTIR spectra of (a) Al_2O_3 (b) PANI (c) Al_2O_3-PANI

XRD Analysis of PANI and Al_2O_3-PANI composite

The XRD of Al_2O_3-PANI composite (Fig. 2b) contains various peaks assigned to alumina[32,33]. The broad peak of PANI[34] (Fig. 2a) centered between 2θ= 20°-30° is reappeared in the XRD of composite. This reveals the interaction of PANI with Al_2O_3[31].

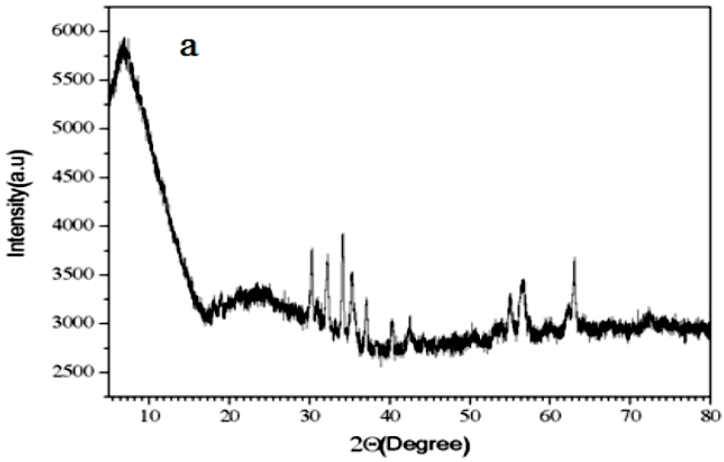

Fig. 2a. XRD spectra of PANI

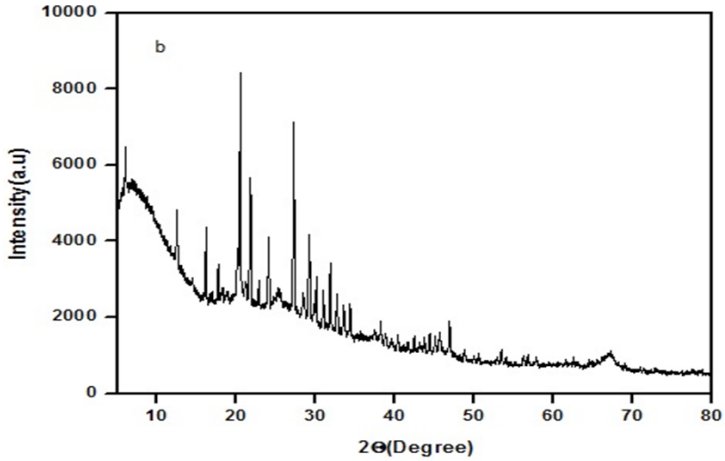

Fig. 2b. XRD spectra of Al_2O_3-PANI composite

SEM Analysis of Al_2O_3 and Al_2O_3- PANI composite

The SEM of metal oxide (Fig. 3a) gazes like a cluster with diameter ranging from 150 nm to 270 nm. The composite SEM (Fig. 3b) display flake structure having diameter ranging from 427 nm to 452 nm. This compeers to the previous work[30,31].

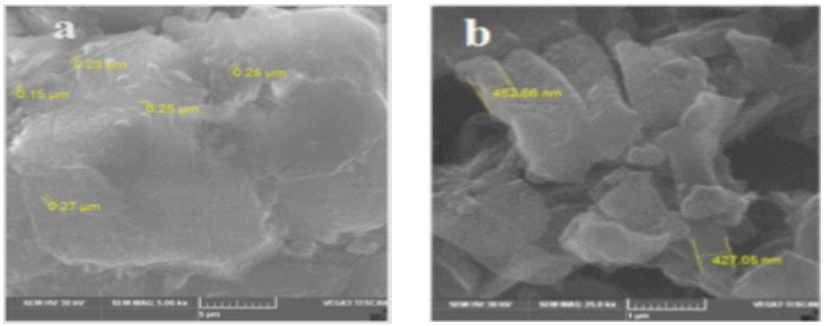

Fig. 3. SEM spectra of (a) Al_2O_3 and (b) Al_2O_3-PANI composite

Preparation of Electrode materials

Specimens fraternized with C: 0.21%, Si: 0.035%, Mn: 0.25%, P: 0.082% and 99.28% of Iron was trimmed into pieces measuring 4 cm x 2 cm x 0.2 cm and were scoured with disparate abrasive sheets starting from 600 grit to 1200 grit. The polished specimens were effaced by double distilled water, acetone and dried in a desiccators. Above freshly polished coupons were utilized in weight loss measurements.

Preparation of Electrolytic solutions

The belligerent solutions of one molar and two molar sulphuric acid were prepared by diluting analytical quality sulphuric acid. Required amount (125-500 ppm) of composite was added to the belligerent solution to obtain test solutions.

Evaluation of inhibition property

Assessment of corrosion by weight loss measurement

Weight loss determination is the preliminary technique to measure corrosion. Freshly polished mild steel coupons were fully immersed in 250 ml of belligerent solutions and test solutions for eight hours continuously under room condition. The coupons were taken out at two hours time intervals, washed with bristle brush under tap water and then cleaned by distilled water, ethyl alcohol and acetone. After drying at room temperature, they were reweighed to assess the inhibition efficiency (IE %) and surface coverage (θ)[35]. The assessed values of IE and (θ) are provided in Table 1 and 2.

Table 1: IE and θ values assessed from the weight loss measurement in 1M belligerent and test solutions

Conc. of Composite (ppm)	2-hours Weight loss (g)	I.E (%)	(θ)	4-hours Weight loss (g)	I.E (%)	(θ)	6-hours Weight loss (g)	I.E (%)	(θ)	8-hours Weight loss (g)	I.E (%)	(θ)
Blank	0.1351	--	--	0.2275	--	--	0.2982	--	--	0.3666	--	--
125	0.0299	78	0.778	0.0534	76	0.765	0.0806	72	0.724	0.108	70	0.705
250	0.0272	80	0.798	0.0484	79	0.787	0.0615	79	0.793	0.0965	73	0.736
375	0.018	87	0.866	0.0332	85	0.854	0.0551	81	0.815	0.093	75	0.746
500	0.0158	88	0.883	0.0301	87	0.867	0.051	82	0.825	0.0715	80	0.804

Table 2. IE and θ values assessed from the weight loss measurement in 2M belligerent and test solutions

Conc. of Composite (ppm)	2-hours Weight loss (g)	I.E (%)	(θ)	4-hours Weight loss (g)	I.E (%)	(θ)	6-hours Weight loss (g)	I.E (%)	(θ)	8-hours Weight loss (g)	I.E (%)	(θ)
Blank	0.2412	--	--	0.4172	--	--	0.5507	--	--	0.7046	--	--
125	0.0748	69	0.689	0.1388	67	0.667	0.1901	65	0.654	0.2609	63	0.629
250	0.0680	72	0.718	0.1261	70	0.697	0.1850	67	0.678	0.2404	65	0.652
375	0.0631	74	0.738	0.1142	72	0.724	0.1668	70	0.698	0.2226	68	0.684
500	0.0522	78	0.783	0.1010	76	0.757	0.1402	74	0.745	0.2016	71	0.714

Attentive examination of the data's existing in the Tables 1 and 2 discloses the substantial conservative nature of Al_2O_3-PANI composite against corrosion. Minimal changes in efficacy observed even after eight hours committed that the prepared water soluble composite have good resistivity versus corrosion.

Open Circuit Potential

The OCP values up to 120 min. were recorded using CHI Electrochemical analyzer 1200B model. A cell comprise of working electrode made from mild steel having 1 cm^2 area, saturated calomel electrode as reference electrode and platinum electrode as counter electrode was employed

to measures the OCP statistics. The perceived information are given in Fig. 4 and 5.

Shift of OCP points to positive potential value on addition of Al_2O_3-PANI composite implies the resistive character[36,28].

Electrochemical measurements

Potentiodynamic polarization and EIS studies were detected in EC-LAB analyzer model 10.37 instrument assembled with three electrode compartment cell. Specimen, having 1cm^2 area and the remaining area covered with araldite epoxy resin, cut from ASTM 415 mild steel was used as working electrode. Calomel electrode and Platinum electrode were used as reference electrode and counter electrode respectively. On maintaining the potential between -200 to +200 m V with scan rate of 0.5m V s^{-1}, the potentiodynamic polarization studies were documented. Impedance measurements were executed with 10 mV AC sine wave amplitude in the frequency range of 100 kHz - 10 mHz.

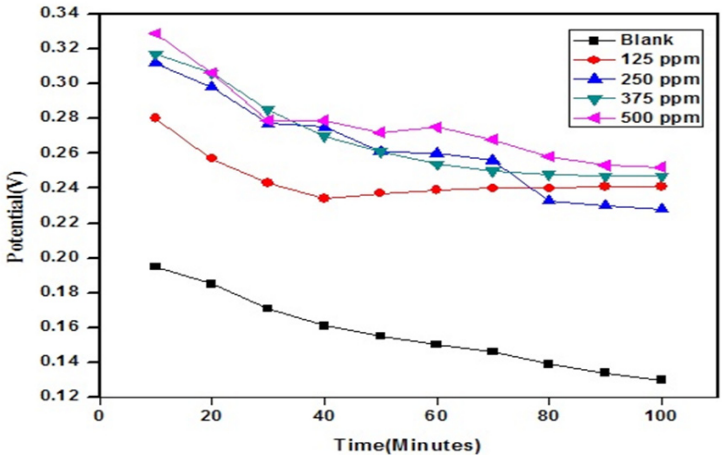

Fig. 4. OCP plot for mild steel in 1 M H_2SO_4

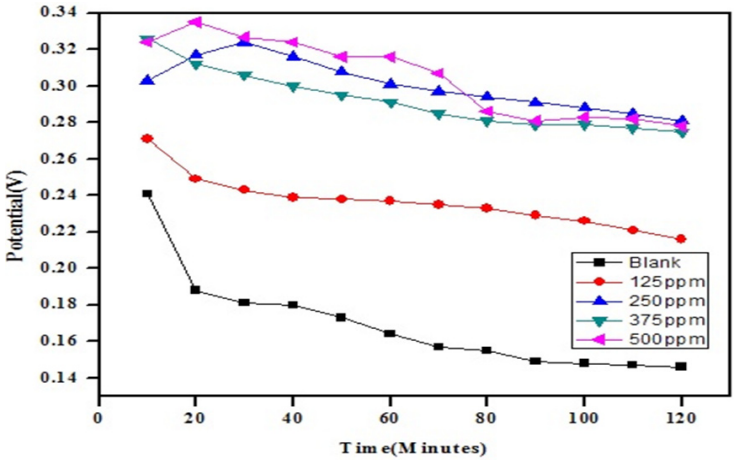

Fig. 5. OCP plot for mild steel in 2 M H_2SO_4

Potentiodynamic polarization measurements

The parameters such as I_{corr}, E_{corr}, b_c and ba and surface coverage (θ) area measured from the Tafel plots given in Fig. 6 and 7 are bestowed in the Table 3 and 4 respectively. Reported formula[37] was used to calculate the resistivity of Al_2O_3-PANI composite.

Increase in corrosion current is noticed with increase in the concentration of acid. The protection accomplishment of the composite is reflected in the steady fall in noticed Icorr value. Changes in efficiency on increasing the I_{corr} concentration of composite undeniably prove the resistivity of the

composite. Inconsiderable changes observed in the E_{corr}, b_a and b_c value presented in Table 3 & 4 on varying the concentration of Al_2O_3-PANI disclose it as mixed type inhibitor[38].

Electrochemical impedance measurements

Impedance parameters (Rct, Cdl) were calculated using the following equivalent circuit.

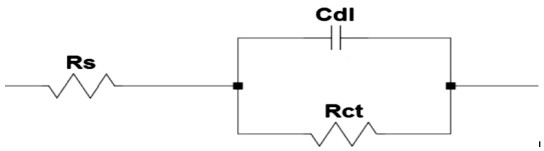

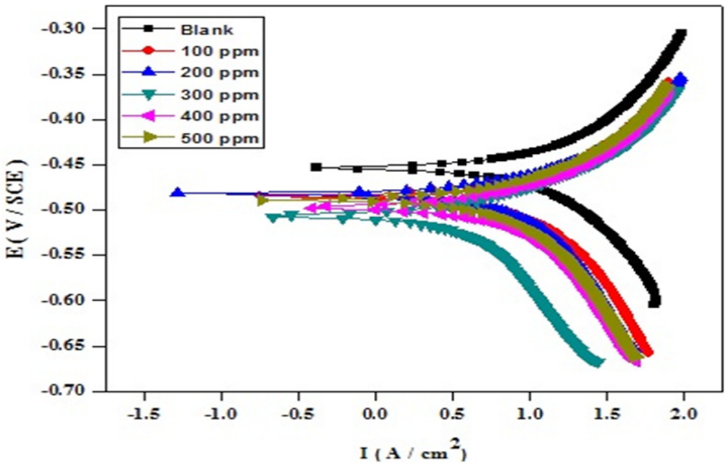

Fig. 6. Tafel plots of mild steel in 1M belligerent and test solutions

Table 3: Corrosion resistive parameters for Mild Steel in 1M belligerent and test solution

Conc. of Composite (ppm)	$-E_{Corr}$ (mV vs. SCE)	b_a (mV dec^{-1})	b_c (mV dec^{-1})	I_{corr} (μA cm^{-2})	Inhibition Efficiency (%)	Surface coverage (θ)
Blank	455	61	63	1960	--	--
100	484	36	40	1269	35	0.3525
200	483	33	37	997	49	0.4913
300	508	33	45	636	67	0.6755
400	496	21	23	616	69	0.6857
500	488	18	20	564	71	0.7122

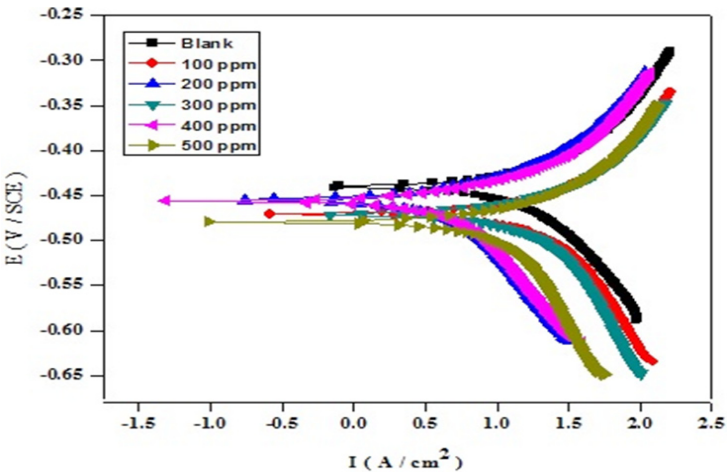

Fig. 7. Tafel plots of mild steel in 2M belligerent and test solutions

Table 4: Corrosion resistive parameters for Mild Steel in 2M belligerent and test solution

Conc. of Composite (ppm)	$-E_{Corr}$ (mV vs. SCE)	b_a (mV dec^{-1})	b_c (mV dec^{-1})	I_{corr} (μA cm^{-2})	Inhibition efficiency (%)	Surface coverage (θ)
Blank	439	44	57	2537	--	--
100	470	24	29	1733	32	0.3169
200	455	48	66	1510	40	0.4048
300	472	20	23	1399	45	0.4485
400	477	20	22	937	63	0.6306
500	480	20	21	904	64	0.6463

Semicircle manifestation of Nyquist plots indicate the protection against corrosion and also reflects single charge transfer process[39]. The decrease in flow of corrosion current reflected in the increase in diameter of capacitive loop. On increasing the concentration of composite, the diameter of the Nyquist plots increases in the Fig. 8 and 9. This reveals that the composite gets adsorbed on the metal surface and prevents the flow of corrosion current and thereby acts as a better inhibitor in low pH environment. Previously reported formula[37] is used to measure the inhibition efficiency.

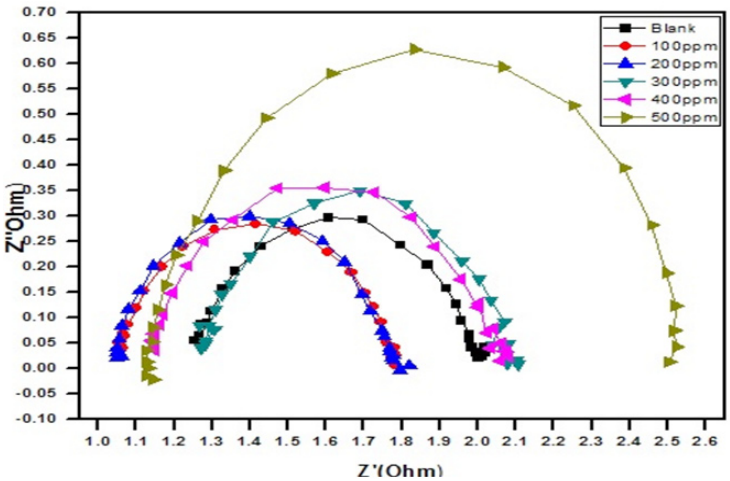

Fig. 8. Cole-Cole plots for mild steel in 1M belligerent and test solution

Table 5: Impedance parameters for Mild Steel in 1M belligerent and test solution

Conc. of Composite (ppm)	R_s (Ω)	C_{dl} (μ F cm^{-2})	R_{ct} (Ω cm^2)	Inhibition efficiency (%)	Surface Coverage (θ)
Blank	1.076	643	0.5018	--	--
100	1.07	712	0.7583	34	0.3417
200	1.278	565	0.8841	38	0.4324
300	1.256	608	0.8961	44	0.44
400	1.153	500	0.9932	50	0.5032
500	1.154	552	1.372	63	0.635

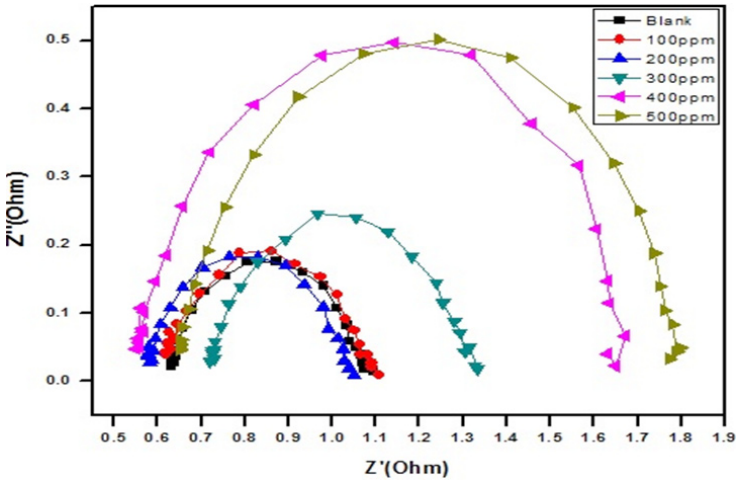

Fig. 9. Cole-Cole plots for mild steel in 2M belligerent and test solution

Table 6: Impedance parameters for mild steel in 2M belligerent and test solution

Conc. of Composite (ppm)	R_s (Ω)	C_{dl} (μ F cm_{-2})	R_{ct} (Ω cm^2)	Inhibition efficiency (%)	Surface Coverage (θ)
Blank	0.6460	1196	0.3773	--	--
100	0.5787	772	0.5945	36	0.3656
200	0.6177	985	0.6168	40	0.3982
300	0.7320	722	0.7212	48	0.4768
400	0.6505	414	1.0076	62	0.6247
500	0.5549	594	1.0080	63	0.6269

The increase in R_{ct} values have been assigned to the formation of protective layer at the metal/electrolyte interface[40]. Decrease in C_{dl} values have been allotted to the increase in thickness of electrical double layer[41]. Reflection of similar behavior in the present observation persist the inhibitive nature of composite.

CONCLUSION

Water soluble PANI coated aluminum oxide composite prepared exhibit good protection efficiency up to 88% in 1M acidic solution for two hours and is stable up to eight hours with little changes in efficiency (80%) on weight loss measurement. Increasing trend of corrosion resistivity upon increasing the concentration of composite is noticed in OCP measurements and electrochemical studies. All observations exposes that synthesized water soluble composite can equipped for industrial maintenance process.

ACKNOWLEDGEMENT

The Authors Acknowledge the support from Dr.B.V., Dean for Research, SRM Group of Institutions, Dr. C. Jayaprabha, Associate Professor of Chemistry, University College of Engineering (Anna University) Dindigul-624622 and the Management of Rajalakshmi Engineering College, Chennai-600 105 for the electrochemical analysis of samples on free of cost. This Research did not receive any specific grant from funding agencies in the public, commercial or not for profit sectors.

REFERENCES

1. Wessling, B.; Passivation of metals by coating with polyaniline: Corrosion potential shift and morphological changes, *Adv. Mater.,* **1994**, *6*, 226-228.
2. Cui, S.; Yin, X.; Yu, Q.; Liu, Y.; Wang, D.; Zhou, F. Polypyrrolenanowire/TiO_2 nanotube nanocomposites as photoanodes for photocathodic protection of Ti substrate and 304 stainless steel under visible light, *Corros. Sci.* **2015**, *98*, 471-477.

3. Kewen Cai,; Shixiang Zuo,; Shipin Luo,; Chao Yao,; Wenjie Liu,; Jianfeng Ma,; Huihui Mao,; Zhongyu Li,; Preparation of polyaniline /graphine composites with excellent anti-corrosion properties and their application in waterborne polyurethane anticorrosive coatings *RSC. Adv*., **2016**, *6*, 95965.
4. Li, H.; wang, X.; Zhang, L.; Hou, B. Preparation and photocathodic protection performance of CdSe/reduced graphene oxide/TiO_2 composite *Corros. Sci*., **2015**, *94*, 342-349
5. Sathiyanarayanan, S.; Syed Azim, S.; Venkatachari, G. Corrosion protection coating containing polyaniline glass flake composite for steel, *Electrochimica Acta.,* **2008**, *53*, 2087–2094.
6. Lebrini, M.; Lagrenée, M.; Traisnel, M.; Gengembre, L.; Vezin, H.; Bentiss, F.; Enhanced corrosion resistance of mild steel in normal sulfuric acid medium by 2,5-bis(n-thienyl)-1,3,4-thiadiazoles: Electrochemical, X-ray photoelectron spectroscopy and theoretical studies, *Applied Surface Science*., **2007**, *253*, 9267-9276.
7. Zhang, F.; Liu, J.; Li, X.; Guo, M.; Study of degradation of organic coatings in seawater by using EIS and AFM methods, *J. Appl. Polym. Sci*., **2008**,*109*,1890-1899.
8. Hongyang, G.; Wei, W.; Likun, X.; Li, M.; Zhangji, Y.; Xiangbo, L. Degradation behavior of a modified epoxy coating in simulated deep-sea environment *J. Chin. Soc. Corrosion Protection.,* **2017**, *37*, 247–263.
9. K.M. Deen, A.F.; Ahmad, R.; Khan, I.H.; Understanding the degradation mechanism of painted steel samples as a function of surface characteristics in artificial sea water *Int. J. Chem. Mater. Sci*., **2013**, *1*, 013–021.
10. Ashraf M.; El Saeed, M.; Abd El-Fattah, M.; Dardir, M.; Synthesis and characterization of titanium oxide nanotubes and its performance in epoxy nanocomposite coating Prog. *Org. Coat*., **2015**, *78*, 83-89.
11. Zhang, X.Z.; Li, Y.J.; Effects of nano-sized titanium powder on the anti-corrosion property of epoxy coatings on steel, *Kem. Ind*., **2014**, *63*, 317-322.
12. Mishra, D.; Anand, S.; Panda 1, R.K.; Das, R.P. Hydrothermal preparation and characterization of boehmites, *Materials Letters*., **2000**, *42*, 38-45.
13. Laachachi, A.; Cochez, M.; Leroy, E.; Gaudon, P.; Ferriol1 M.; Lopez Cuesta, J. M. Effect of Al_2O_3 and TiO_2 nanoparticles and APP on thermal stability and flame retardance of PMMA, *Polym. Adv. Technol.,* **2006**, *17*, 327-334.
14. Christophe Ne´dez,; Jean-Paul Boitiaux,; Charles J.; Cameron,; Blaise Didillon, Optimization of the Textural Characteristics of an Alumina To Capture Contaminants in Natural Gas, *Langmuir*., **1996**, *12*, 3927-3931.
15. Zhanhu Guo,; Tony Pereira,; Oyoung Choi,; Ying Wang,; H. Thomas Hahn,; Surface functionalized alumina nanoparticle filled polymeric nanocomposites with enhanced mechanical properties, *J. Mater. Chem*., **2006**, *16*, 2800-2808.
16. Alan G. MacDiarmid, Arthur J. Epstein, Polyanilines: a novel class of conducting polymers, Faraday Discuss. *Chem. Soc*., **1989**, *88*, 317-332.
17. Li, X.W.; Li, X.H.; Dai, N.; Wang, G.C.; Wang, Z. Preparation and electrochemical capacitance performances of super-hydrophilic conducting polyaniline, *J. Power. Sources*., **2010**, *195*, 5417-5421.
18. Jiaxing Huang, Shabnam Virji, Bruce H. Weiller, Richard B. Kaner, Polyaniline Nanofibers: Facile Synthesis and Chemical Sensors, *J. Am. Chem. Soc*., **2003**,*125*, 314-315.
19. Xia, H.; Wang, Q.; Ultrasonic Irradiation: A novel approach to prepare conductive polyaniline/ nanocrystalline titanium oxide composites *Chem. Mater.,* **2002**,*14*, 2158-2165.
20. Teoh, G. L.; Liew, K. Y.; Mahmood, Wan A. K. Preparation of polyaniline-Al_2O_3 composites nanofibers with controllable conductivity, *Mater. Lett.* **2007**, *61*, ,4947- 4949.
21. J. Zhu, S. Wei, L. Zhang, Y. Mao, J. Ryu, N. Haldolaarachchige, D.P. Young, Z. Guo, Electrical and dielectric properties of polyaniline-Al_2O_3 nanoparticles derived from various Al_2O_3 nanocomposite, *J. Mater. Chem*., **2011**, *21*, 3952–3959.
22. Ahlatcioglu, E.; Celik Bozdogan, A.; Filiz Senkal, B.; Okutan, M.; The effect on the impedance characteristics of the metal oxide (Al_2O_3 and ZnO) doping in to polyaniline, *Material Science in Semiconductor Processing*

2016, *56*, 357-561.

23. Kamatchi Selvaraj, P.; Sivakumar, S.; Selvaraj, S.; NiO-PANI composite as potential inhibitor for Mild Steel in acidic corrosion environment *Int. J. chem. sci.*, **2018**, *16*(2) 268.
24. Sivakumar, S.; Kamatchi Selvaraj, P.; Selvaraj, S.; Inhibition Efficiency of water Soluble Sr(ZnZr)1Fe10O19-PANI Composite against Strong acidic condition for Mild Steel, accepted for publication in *Asian journal of chemistry*., **2018**, *30* ISSN 2043-2048.
25. Sivakumar, S.; Kamatchi Selvaraj, P.; Selvaraj, S.; Adsorption effect of simple metal oxide composite (CuO-PANI) on corrosion behavior of Mild Steel in low pH medium, *Journal of Electrochemical Science and Technology* **2018** under review.
26. Majid Farahmandjou,; Nazafarin Golabiyan,; New pore structure of nano-alumina (Al_2O_3) prepared by sol gel method, *Journal of Ceramic Processing Research*., **2015**, *16* (2) 1-4.
27. Manyasree D. A,; Kiranmayi P.; A, Ravi Kumar R.; V. S. S. N. B, Synthesis, Characterization And Antibacterial Activity Of Aluminium Oxide Nanoparticles, *Int J Pharm Pharm Sci*., **2018**, *10*, 32-35.
28. Sathiyanarayanan, S.; Syed Azim, S.; Venkatachari, G., A new corrosion protection coating with polyaniline-TiO_2 composite for steel, *Electrochimica Acta* **2007**, *52*, 2068-2074.
29. Yuetao Yi,; Guangyang Liu,; Zhining Jin,; Dawei Feng,; The use of conducting Polyaniline as Corrosion Inhibitor for Mild Steel in Hydrochloric Acid, *Int. J. Electrochem. Sci*., **2013**, *8*, 3540-3550.
30. Zhu, J.; Wei, S.; Zhang, L.; Mao, Y.; Ryu, J.; Haldolaarachchige, N.; Young, D.P.; Guo, Z. Electrical and dielectric properties of polyaniline–Al_2O_3 nanocomposites derived from various Al_2O_3 nanostructures *J. Mater. Chem*., **2011**, *21*, 3952-3959.
31. Ahmed A. Ahmed Al-Dulaimi,; Shahrir Hashim,; Mohammed Ilyas Khan,; Corrosion Protection of Carbon Steel Using Polyaniline Composite with Aluminium Oxide, Pertanika *J. Sci. & Technol*., **2011**, *19*, 329-337.
32. Tawfik A Saleh.; Vinod K Gupta,; Synthesis and Characterization of alumina nano- particles Polyamide membrane with enhanced flux rejection performance, separation and *Purification Technology.,* **2012**, *89*, 245-251.
33. Shek, C.H.; Lai, J.K.L.; Transformation Evolution And Infrared Absorption Spectra of Amorphous And Crystalline Nano-Al_20_3 Powders, *Nanostructure Mateds*., **1997**, *8*, 605-610.
34. XiaominCai,; Xiuguo Cui,; Lei Zu,; You Zhang,; XingGao,; Huihin Lian,; Yang Liu Xiaodong wang, Ultra High Electrical Performance of Nano nickel oxide and polyaniline composite, *Polymer*., **2017**, *9*, 288.
35. Ashish kumar Singh, Quraishi, M.A.; The effect of some bis-thiadiazole derivatives on the corrosion of mild steel in hydrocholoric acid, *Corrosion Science*., **2010**, *52*, 1373-1385.
36. Wessling, B.; Posdorfer, J.; Corrosion prevention with an organic metal (polyaniline): corrosion test results *Electrochim Acta*., **1999**, *44*, 2139.
37. Yaser Jafari, Sayed Mehdi Ghoreishi, Mehdi Shabani-Nooshabadi, Electrochemical deposition and characterization of polyaniline-graphene nanocomposite films and its corrosion protection properties *J. of Polym. Res*., **2016**, *23*, 91.
38. Jayaprabha, C.; Sathiyanarayanan, S.; Venkatachari, G.; Polyaniline as Corrosion inhibitior for iron in Acid Solutions, *J. of Applied Surface Polymer Science.,* **2005**, *101*, 2144-2153.
39. Mansfeld, F.; Kendig, M. W.; Tsai, S.; Recording and Analysis of AC Impedance Data for Corrosion Studies *Corrosion.,* **1982**, *38*, 570-580.
40. Yujie Qiang,; Shengtao Zhang,; Shenying Xu,; Wenpo L, Experimental and theoretical studies on the corrosion inhibition of copper by two indazole derivatives in 3.0% NaCl solution *J. of Colloid and interface science .,* **2016**, *472*, 52-59.
41. Lukman Olasunkanmi,; Ime Bassey Obot,; Mwadham M Kabanda,; Eno E. Ebenso, Some Quinoxalin-6-yl derivatives as Corrosion Inhibitors for Mild Steel in Hydrochloric Acid: Experimental and Theoretical Studies, *J. Phys. Chem*. **2015**, *119*(28), 16004-1601.